Localization of 3D Ambisonic Recordings and Ambisonic Virtual Sources

Sebastian Braun and Matthias Frank
Universität für Musik und darstellende Kunst Graz, Austria
Institut für Elektronische Musik und Akustik, Email: frank@iem.at

Abstract

The accurate recording and reproduction of real 3D sound environments is still a challenging task. In this paper, the two most established 3D microphones are evaluated: the Soundfield SPS200 and MH Acoustics' Eigenmike EM32, according to 1st and 4th order Ambisonics. They are compared to virtual encoded sound sources of the same orders in a localization test. For the reproduction, an Ambisonics system with 24 (12+8+4) hemispherically arranged loudspeakers is used. In order to compare to existing results from the literature, this paper focuses on sound sources in the horizontal plane. As expected, the 4th order sources yield better localization as the 1st order sources. Within each order, the real recordings and the virtual encoded sources show a good correspondence.

Introduction

Surround sound systems have entered movie theaters and our living rooms during the last decades. But these systems are still limited to horizontal sound reproduction. Recently, further developments, such as 22.2 [1] and AURO 3D [2], expanded to the third dimension by adding height channels.

The third dimension envolves new challenges in panning and recording [3]. VBAP [4] is the simplest method for panning and at the same time the most flexible one, as it works with arbitrary loudspeaker arrangements. But as the mixed signals can only be stored in discrete channels according to the loudspeaker arrangement, a mix-down is problematic as a delivery format. Multichannel recording for pair-/tripletwise mapping on loudspeakers is similar: The microphone arrangement has to be adapted to the loudspeaker arrangement. This means, that an explicit recording has to be done for each possible loudspeaker arrangement that might be used for the playback.

So it is desirable to do one single recording that can be decoded to arbitrary loudspeaker arrangements. This is one concept behind Ambisonics [5]. Newer developments of Ambisonics offer a high spatial resolution [6, 7] and the capability of using arbitrary loudspeaker arrangements for playback [8, 9].

This paper investigates two available microphone arrays for Ambisonic recording and compares the perceived localization to virtual encoded (= amplitude-panned) sources in a listening test. In the test, a hemispherical arrangement of 24 loudspeakers is used for the reproduction.

The paper is arranged as follows: It gives a brief overview of Ambisonics, its encoding and decoding. The subsequent section describes the two used mircophone arrays and the measurment of the spatial impulse responses for the creation of the stimuli. After that, we explain the method, the conditions, and the setup of the subjective localization test. Finally, the results are presented, discussed, and compared to what is known from literature.

Coordinate system. Fig. 1 shows the coordinate system used in this paper. The directions $\boldsymbol{\theta}$ are vectors of unit length that depend on the azimuth angle φ and zenith angle ϑ ($\vartheta = 90°$ in the horizontal plane)

$$\boldsymbol{\theta}(\varphi, \vartheta) = \begin{pmatrix} \cos(\varphi)\sin(\vartheta) \\ \sin(\varphi)\sin(\vartheta) \\ \cos(\vartheta) \end{pmatrix}. \tag{1}$$

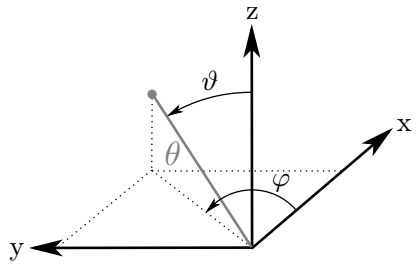

Figure 1: Spherical coordinate system.

Ambisonics

Ambisonics is a 3D recording and reproduction method which is based on the representation of the sound field as a superposition of orthogonal basis functions. These basis functions are the solutions of the Helmholtz-equation (lossless, linear wave equation in the frequency domain) in the spherical coordinate system and they are called spherical harmonics. The spherical harmonics up to the order N = 4 are depicted in Fig. 2. They are labeled by two indices: n determines how many nodal circles the spherical harmonic modes have, and $|m|$ (m runs from $-n$ to n) counts how many of them run through the North and South pole. They maximum order N determines the spatial resolution and the number $(\mathrm{N}+1)^2$ of signals.

Encoding. A source distribution $f(kr, \boldsymbol{\theta})$ on a sphere can be represented as

$$f(kr, \boldsymbol{\theta}) = \sum_{n=0}^{\mathrm{N}} \sum_{m=-n}^{n} \phi_n^m(kr)\, Y_n^m(\boldsymbol{\theta}). \tag{2}$$

The resulting coefficents $\phi_n^m(kr)$ describe a spherical spectrum. The assumption that all sources in the sound field and the reproduction system lie on a sphere of the same radius r yields a frequency independent processing. For one source at $\boldsymbol{\theta}_s$, the Ambisonic signals $\boldsymbol{\phi}_{\mathbf{N}}^{(\mathrm{virt})}$ can be computed by evaluating the spherical harmonics for $\boldsymbol{\theta}_s$ and multiplication with the signal s:

$$\boldsymbol{\phi}_{\mathbf{N}}^{(\mathrm{virt})}(\boldsymbol{\theta}_s) = (Y_0^0(\boldsymbol{\theta}_s), Y_1^{-1}(\boldsymbol{\theta}_s), ...Y_{\mathrm{N}}^{\mathrm{N}}(\boldsymbol{\theta}_s)) \cdot s. \quad (3)$$

This source type is used for all virtual sources in this paper.

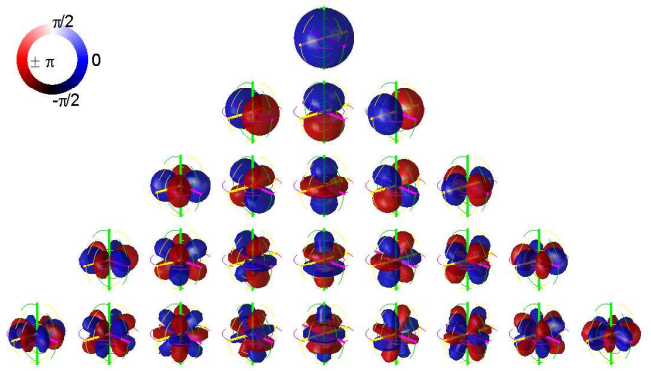

Figure 2: Real-valued spherical harmonics $Y_n^m(\boldsymbol{\theta})$. Rows correspond to orders $0 \leq n \leq 4$, columns to degrees $-n \leq m \leq n$.

Ambisonic Recording. In order to compute the Ambisonic signals from a recording, all the M sensor positions $\boldsymbol{\theta}_m$ on the microphone array have to be considered. A matrix expressing all sensor positions in Ambisonics results in $\boldsymbol{Y}_{\mathbf{N}} = (\boldsymbol{y}_{\mathbf{N}}(\boldsymbol{\theta}_1), \boldsymbol{y}_{\mathbf{N}}(\boldsymbol{\theta}_2), ...\boldsymbol{y}_{\mathbf{N}}(\boldsymbol{\theta}_{\mathrm{M}}))$, with $\boldsymbol{y}_{\mathbf{N}}(\boldsymbol{\theta}_m) = (Y_0^0(\boldsymbol{\theta}_m), Y_1^{-1}(\boldsymbol{\theta}_m), Y_1^0(\boldsymbol{\theta}_m), ...Y_{\mathrm{N}}^{\mathrm{N}}(\boldsymbol{\theta}_m))$. The M sensor signals $\boldsymbol{p} = (p_1, p_2, ...p_{\mathrm{M}})$ yield the intermediate Ambisonic signals $\hat{\boldsymbol{\phi}}_{\mathbf{N}}$ by matrix inversion of $\boldsymbol{Y}_{\mathbf{N}}$:

$$\hat{\boldsymbol{\phi}}_{\mathbf{N}}^{(\mathrm{mic})} = \boldsymbol{Y}_{\mathbf{N}}^{\dagger} \cdot \boldsymbol{p}. \quad (4)$$

The highest possible order $\mathrm{N}_{\mathrm{max}}$ is dependent on the number of sensors M:

$$\mathrm{N}_{\mathrm{max}} \leq \sqrt{\mathrm{M}} - 1. \quad (5)$$

For rigid sphere microphone arrays, such as the Eigenmike used in this study, the signals $\boldsymbol{p}$ usually express the sound pressure picked up by the sensors. The radius of the microphone array is much smaller than the radius of the loudspeaker arrangement for playback. This results in a strong attenuation of the signals associated with low frequencies and high orders. Thus, the Ambisonic signals $\hat{\boldsymbol{\phi}}_{\mathbf{N}}^{(\mathrm{mic})}$ of the recordings have to be adapted prior to the playback. This can be done by filters which compensate for the radial propagation from the playback arrangement to the radius of the microphone array. A practical implementation of these radial filters with regard to the signal-to-noise ratio of the microphone array can be found in [10]. The filtering of $\hat{\boldsymbol{\phi}}_{\mathbf{N}}^{(\mathrm{mic})}$ yields the Ambisonic signals $\boldsymbol{\phi}_{\mathbf{N}}^{(\mathrm{mic})}$ that are applicable for playback.

For noise-free recordings of point sources in an anechoic chamber with microphone arrays of perfectly matching and accurately placed sensors, $\boldsymbol{\phi}_{\mathbf{N}}^{(\mathrm{mic})}$ equals the Ambisonic signals for a virtual source $\boldsymbol{\phi}_{\mathbf{N}}^{(\mathrm{virt})}$ at the same position. The listening test evaluates the effect of practical array imperfections.

Decoding. The decoder derives the signals $\boldsymbol{g} = \{g_1, ...g_{\mathrm{L}}\}$ for the L loudspeakers of an arrangement from the Ambisonic signals $\boldsymbol{\phi}_{\mathbf{N}}$ by multiplying with the decoder matrix $\boldsymbol{D}$:

$$\boldsymbol{g} = \boldsymbol{D}\, \boldsymbol{\phi}_{\mathbf{N}}. \quad (6)$$

The same decoding holds for recordings $\boldsymbol{\phi}_{\mathbf{N}}^{(\mathrm{mic})}$ and virtual sources $\boldsymbol{\phi}_{\mathbf{N}}^{(\mathrm{virt})}$. The computation of a suitable decoder matrix is a challenging task, especially if the loudspeakers cover only a part of a sphere. Possible solutions can be found in [8, 9].

Microphone arrays

Two different commercially available microphone arrays are used in this study. The *Soundfield SPS 200* and *MH Acoustics' Eigenmike EM32*.

(a) Soundfield SPS200 (b) Eigenmike EM32

Figure 3: Picture of the two used microphone arrays.

Soundfield SPS200. The Soundfield SPS200 is built of 4 sensors with cardioid characteristic, placed on the vertices of a tetrahedron. The sensor signals were amplified with a SMP200 4-channel preamp, which offers global gain control. With the provided VST plugin, it is possible to convert the 4 separate tracks (so-called Ambisonics A-format) into other formats such as 5.1 Surround, several 1st order directivity patterns, and 1st order Ambisonics (so-called B-format). As we used this microphone array as the representative for 1st order Ambisonics in the evaluation, we chose the latter possibility to create the Ambisonic signals $\boldsymbol{\phi}_{\mathbf{N}}^{(\mathrm{mic})}$.

Eigenmike EM32. The Eigenmike EM32 has 32 omni-directional sensors, placed on the surfaces of a truncated icosahedron (soccer ball) with a radius of 4.2 cm. The microphone array is equipped with built-in preamps and A/D converters. According to Eq. (5), the 32 sensor signals can be converted into Ambisonics signals with a maximum order of 4. We chose to exploit the maximum order and used this microphone array as the representative for 4st order Ambisonics in the evaluation. The above-mentioned radial filters are applied to the signals to achieve $\boldsymbol{\phi}_{\mathbf{N}}^{(\mathrm{mic})}$.

Measurement of spatial impulse responses. Instead of recording the desired stimuli directly, spatial impulse responses (with 4 or 32 channels respectively) for several directions $\boldsymbol{\theta}$ were measured. For both microphone arrays, the measurement took place under the same conditions, but seperately. We used exponential sweeps with a length of 1 s at a sampling rate of 44.1 kHz, played back over a 1-way loudspeaker at a distance of 1 m to the microphone array under test. The microphone array was set up in the origin of the coordinate system. Thus, the azimuth angles φ of the directions $\boldsymbol{\theta}$ could be measured directly using an angle measurement tool with laser beam. The elevation angles ϑ were derived from the distance relations between microphone array and loudspeaker.
For this study, it was desirable to measure under free-field conditions, that is to ensure that the influence of the measurement room is negligible. In order to suppress reflections, the impulse responses were windowed to 20 samples, which equals approximately the time of the diffraction path around the Eigenmike.

Evaluation Method

The localization of the two microphone arrays is evaluated in a subjective listening test and compared to virtual sources of the same orders (1st and 4th). For the 4th order we tested 30 and for the 1st order 25 directions. The directions $\boldsymbol{\theta}$ of the recordings and virtual sources are the same within each order. As control conditions, we added 5 single loudspeakers. This yields 115 conditions per subject, which were presented in random order.

For each condition, the Ambisonic signals $\boldsymbol{\phi}_{\mathbf{N}}^{(\mathrm{mic})}$ and $\boldsymbol{\phi}_{\mathbf{N}}^{(\mathrm{virt})}$ respectively, were convolved with pink noise bursts in 5 segments of 200 ms. All stimuli were reproduced by an Ambisonics system with 24 loudspeakers distributed on a hemishpere in 3 rows (see Tab. 1). The used decoder is optimized for loudspeaker systems, which cover only parts of the sphere [8]. The energy from the non-existent lower hemisphere is mainly preserved by the loudspeakers in the horizontal plane. The delay and gain differences of all loudspeaker were compensated for the listening position. The reproduction system is installed in the IEM CUBE, a 11 m x 11 m x 5 m room with a reverberation time $\mathrm{RT}_{60} < 1$ s. In order to avoid disturbing effects from floor reflections, the area around the listener was prepared with heavy molleton over chairs, see Fig. 4.

l	φ_l in °	ϑ_l in °	l	φ_l in °	ϑ_l in °
1	0	90.0	13	22.7	61.5
2	23.7	89.5	14	67.9	61.5
3	48.2	89.4	15	114.2	62.1
4	72.6	89.3	16	157.8	61.3
5	103.1	89.4	17	-156.4	61.3
6	138.5	89.8	18	-113.3	61.6
7	179.8	89.6	19	-65.4	61.5
8	-138.3	89.9	20	-22.7	62.0
9	-100.9	89.4	21	46.8	33.0
10	-69.8	89.6	22	133.4	33.0
11	-44.8	89.5	23	-133.4	33.4
12	-21.4	89.5	24	-43.4	32.3

Table 1: Azimuth angles φ_l and zenith angles ϑ_l of the used 12+8+4 loudspeaker arrangement.

Figure 4: Subject during the listening test, pointing towards the perceived direction.

The subjects could start the stimulus playback by themselves and repeat it as often as they wanted. During listening, they had to face the 0° direction. After listening, they were pointing towards the perceived direction $\boldsymbol{\theta}_{\mathrm{p}}$ with a toy-gun as pointing device [11]. The position and orientation of the pointing device was captured by an infrared tracking system (see Fig. 4). The resulting direction was stored when subjects pulled the trigger of the toy-gun. The listening test was carried out with 10 subjects. All of them are experienced listeners and have no hearing impairments.

Results

For the evaluation, some variables are introduced. φ_{t} and ϑ_{t} denote the target azimuth and zenith angle. The corresponding perceived azimuth and zenith angles are φ_{p} and ϑ_{p}. The angle errors e_φ and e_ϑ are defined as

$$e_\varphi = (\varphi_{\mathrm{p}} - \varphi_{\mathrm{t}}) \bmod 360° \quad \text{and} \quad e_\vartheta = \vartheta_{\mathrm{p}} - \vartheta_{\mathrm{t}}. \tag{7}$$

The target directions $\boldsymbol{\theta}_{\mathrm{t}}$ and perceived directions $\boldsymbol{\theta}_{\mathrm{p}}$ are composed from their corresponding azimuth and zenith angles according to Eq. (1). The direction error e_{dir} is defined as the deviation of the perceived direction $\boldsymbol{\theta}_{\mathrm{p}}$ from the target direction $\boldsymbol{\theta}_{\mathrm{t}}$:

$$e_{\mathrm{dir}} = \arccos(\langle \boldsymbol{\theta}_{\mathrm{t}}, \boldsymbol{\theta}_{\mathrm{p}} \rangle). \tag{8}$$

Direction error. The direction error e_{dir} for the 5 single loudspeakers showed no subjective dependency and a median value of 4.4°. Thus, no subjects were excluded from the evaluation. Since sometimes front-back confusions were perceived by the subject, azimuth angles with $|e_\varphi| > 120°$ are mostly excluded from the analysis and treated seperatly (see Tab. 2).
Fig. 5 shows the direction error, which is much smaller for the Eigenmike and 4$^{\mathrm{th}}$ order virtual sources than for the Soundfield and the 1$^{\mathrm{st}}$ order virtual sources. Within each order, the errors of the virtual sources are smaller. An ANOVA showed significant differences between all mean values, but the median values of the Eigenmike and 4$^{\mathrm{th}}$ order virtual sources are not significantly different.
In order to get a more detailed view, the following paragraphs examine azimuth and zenith angle errrors seperatly.

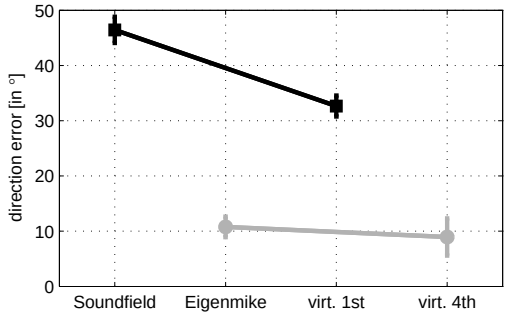

Figure 5: Medians of the direction error e_{dir} and corresponding 95 % CI.

Azimuth angle error in the horizontal plane. Figs. 6 and 7 show the relation between the target azimuth angle φ_{t} and the perceived azimuth angle φ_{p} in the horizontal plane. The markers are based on histograms of φ_{p} for each φ_{t}, changing their size depending on the number of holding data points. The median is drawn as solid line and a reference ideal median as dashed line. The histograms use all data points, whereas the medians are calculated excluding front-back confusions ($|e_\varphi| > 120°$).
Regarding the medians, the Eigenmike and 4$^{\mathrm{th}}$ order virtual sources yield similar results: For each direction, the median of the perceived angles is close to the target angle. The 1$^{\mathrm{st}}$ order conditions (Soundfield and 1$^{\mathrm{st}}$ order virtual) show greater deviations from the target angles. The perception of lateral sources shows a drift towards 180°. Within the each order, the median values of recordings and virtual sources are comparable.

Front-back confusions. Tab. 2 shows the relative amount of front-back confusions in the horizontal plane. The amount of front-back confusions depends on the Ambisonics order: It decreases with increasing order. Comparing the recordings with their corresponding virtual sources, the recordings yield a higher amount of front-back confusions.

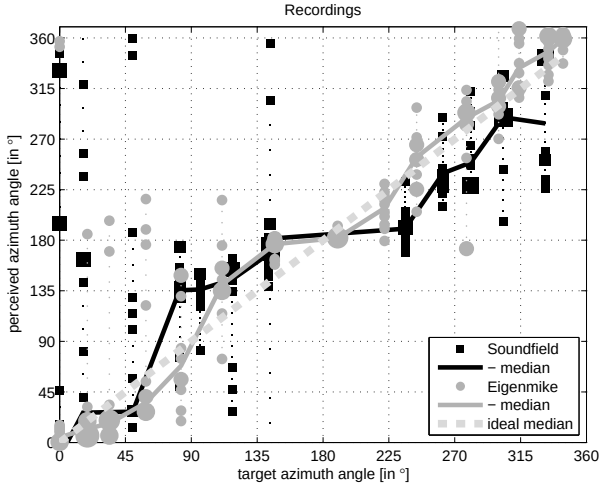

Figure 6: Azimuth angle mapping φ_{t} vs. φ_{p} in the horizontal plane for recordings: histogram for each target angle φ_{t}, marker size indicates number of values, lines show corresponding medians, medians exclude front-back confusions ($|e_\varphi| > 120°$).

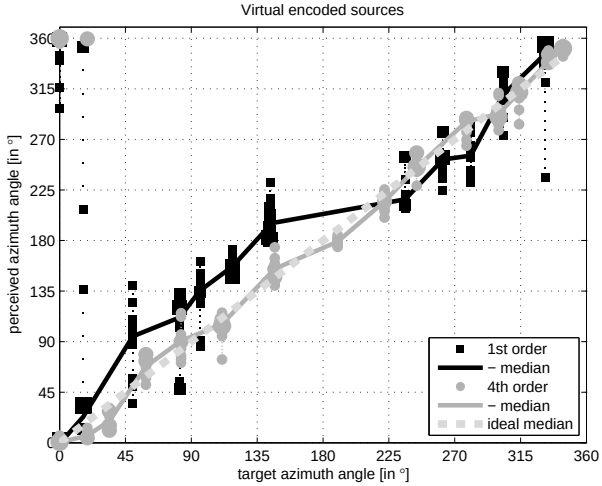

Figure 7: Azimuth angle mapping φ_{t} vs. φ_{p} in the horizontal plane for virtual sources: histogram for each target angle φ_{t}, marker size indicates number of values, lines show corresponding medians, medians exclude front-back confusions ($|e_\varphi| > 120°$).

front-back confusions	%
Soundfield	10.6
virtual 1$^{\mathrm{st}}$ order	1.7
Eigenmike	4.0
virtual 4$^{\mathrm{th}}$ order	0.0

Table 2: Relative amount of front-back confusions ($|e_\varphi| > 120°$) in the horizontal plane.

Zenith angle error. Fig. 8 shows the absolute zenith error for three groups of zenith angles: zenith target angles ϑ_{t} in and slightly over the horizontal plane [90° 60°[, near the North pole [30° 0°], and between [60° 30°[. The error of the Eigenmike recordings increases towards the North pole, while this tendency is weak for the 4$^{\mathrm{th}}$ order virtual sources. The increase of the

zenith angle error towards the North pole corresponds to psychoacoustic findings [12], which report also an underestimation of the elevation for sources near the North pole. Interestingly, the errors of the Soundfield and 1st order virtual sources hold the highest values in the horizontal plane and decrease towards the North pole.

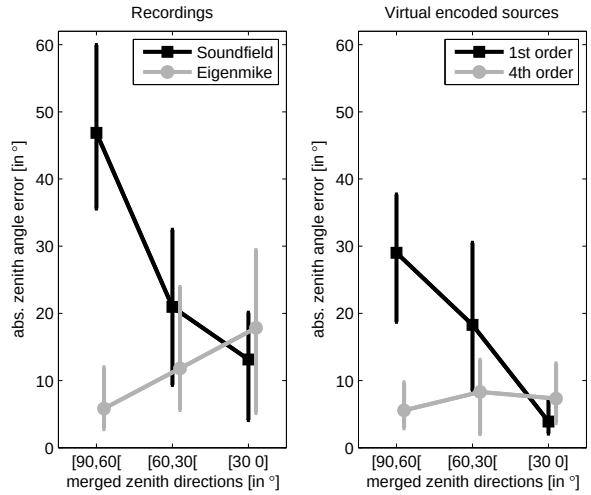

Figure 8: Absolute zenith angle error $|e_\vartheta|$ for recordings and virtual encoded sources of 1st and 4th order. Directions are merged into 3 groups. Markers indicate medians and errorbars the inter-quartile ranges.

For further analysis of this observation, Fig. 9 investigates the orientation of the zenith angle error. The 4th order sources show the known underestimation of the elevation for sources near the North pole. The high values of the absolute zenith angle error for the 1st order sources in the horizontal plane are due to the overestimation of the elevation, which decreases towards the North pole.

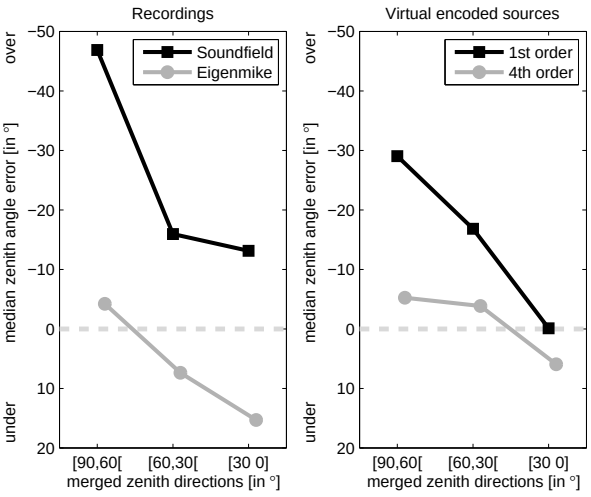

Figure 9: Medians of zenith angle error e_ϑ for recordings and virtual encoded sources of 1st and 4th order. Directions are merged into 3 groups.

Discussion

The results show that the localization errors are strongly dependent on the Ambisonics order. This dependency is also known from literature about 2D (horizontal-only) Ambisonics [13, 14]. In [13], Bertet found that the localization accuracy of 4th order recordings (using an array with 32 sensors) and virtual sources is comparable. This is approved also for the 3D case by our results. Bertet obtained a median localization error of 5° using 4th order 2D Ambisonics, while in our 3D case the direction error yields about 10°. As the direction error e_{dir} incorporates both azimuth and zenith angle errors, the results are not directly comparable.

The drift towards the rear for lateral sources in the horizontal plane that is observed in our experiment, can be also found in the article of Bertet. The same article reports a high number of front-back confusions for the Soundfield recordings, like in our results.

When listening to single sources, the zenith angle error is the smallest in the horizontal plane and increases towards the North pole, where the elevation is underestimated [12]. This holds also for the 4th order sources in our experiment. In contrast, the elevation of 1st order sources in the horizontal plane is overestimated. The overestimation decreases towards the North pole. This behaviour is a superposition of two effects: the first one is the above-mentioned underestimation of the elevation towards the North pole and the second one is caused by the reproduction setup. In a full-sphere Ambisonics reproduction setup, also loudspeakers above and below the horizontal plane contribute to sources in the horizontal plane. The lower the order, the bigger is the active loudspeaker area. If the lower hemisphere is non-existent, sources in the horizontal plane are perceived elevated. Of course, this elevation depends on the Ambisonics order. The used decoder preserves the energy of the lower hemisphere by increasing the level of the loudspeakers in the horizontal plane. Other decoders may cause even a stronger elevation drift using a hemispherical reproduction setup. Possible solutions to reduce this drift could also be the use of less loudspeakers for low orders, a spatial sharpening of low order sources [15], or Ambisonics warping [16].

There are no directly comparable studies for 3D localization in Ambisonics available in literature. Pulkki [17] did a similar experiment using VBAP. But the results were only comparable, if the experiments would have used the same loudspeaker setup.

Conclusion

This paper evaluates the subjective localization of the Soundfield SPS200 and MH Acoustics' Eigenmike EM32 and compares them to virtual encoded sound sources of 1st and 4th order, using a hemispherical Ambisonics reproduction setup. The results show that the localization accuracy is mainly dependent on the Ambisonics order: the higher the order, the better the localization.

Within the 1st order, the virtual sources yield a better localization than the Soundfield recordings. The 4th order virtual sources and the Eigenmike recordings are comparable.
The results in the horizontal plane show similar tendencies as 2D experiments from the literature. While the localization of the elevation angle using 4th order follows psychoacoustical findings for single sound sources, the localization using 1st order is additionally influenced by the reproduction setup.
Summarizing, the microphone arrays show localization properites according to their Ambisonics order. The Eigenmike offers a possiblity for 3D recordings with good spatial resolution. Still, the evaluation of real musical recordings is an open but promising task.

Acknowledgements

We thank all subjects for their participation in the listening test and Franz Zotter for helpful suggestions.

References

[1] K. Hamasaki, K. Hiyama, R. and Okumura: "The 22.2 multichannel sound systems and its application," AES 118th Convention, Barcelona, Spain, 2005.

[2] Auro technology Auro 3D speaker layouts. URL: `http://www.auro-3d.com/general-highlights/speaker-layout?section=Consumer`.

[3] G. Theile and H. Wittek: "Principles in Surround Recordings with Height," AES 130th Convention, London, UK, 2011.

[4] V. Pulkki: "Virtual Sound Source Positioning Using Vector Base Amplitude Panning," J. Audio Eng. Soc., Vol. 45, No. 6, 1997.

[5] M. A. Gerzon: "Periphony: With-Height Sound Reproduction," J. Audio Eng. Soc., Vol. 21, No. 1, 1973.

[6] J. Daniel: "Représentation de Champs Acoustiques, Application à la Transmission et à la Reproduction de Scènes Sonores Complexes dans un Contexte Multimédia," Dissertation, Université de Paris 6, Paris, France, 2001.

[7] F. Zotter, H. Pomberger, and M. Frank: "An Alternative Ambisonics Formulation: Modal Source Strength Matching and the Effect of Spatial Aliasing," AES 126th Convention, Munich, Germany, 2009.

[8] F. Zotter, M. Frank, and A. Sontacchi: "The Virtual T-Design Ambisonics-Rig Using VBAP," EAA Euroregio 2010, Ljubljana, Slovenia, 2010.

[9] F. Zotter, H. Pomberger, and M. Noisternig: "Energy preserving Ambisonic decoding," Acta Acustica united with Acustica, accepted for publication, Jan. 2012.

[10] R. Baumgartner, H. Pomberger, and M. Frank: "Practical Implementation of Radial Filters for Ambisonic Recordings," ICSA 2011, Detmold, Germany, 2011.

[11] M. Frank et al.: "Flexible and intuitive pointing method for 3D auditory localization experiments," AES 38th International Conference, Pitea, Sweden, 2010.

[12] J. Blauert: "Spatial Hearing - The Psychophysics of Human Sound Localization," The MIT-Press, Cambridge, MA, 1983.

[13] S. Bertet et al.: "Investigation of the perceived spatial resolution of higher order Ambisonic sound fields: A subjective evaluation involving virtual and real 3D microphones," AES 30th International Conference, Saariselkä, Finland, 2007.

[14] M. Frank, F. Zotter, and A. Sontacchi: "Localization Experiments Using Different 2D Ambisonics Decoders," 25th TMT VDT International Convention, Leipzig, Germany, 2008.

[15] V. Pulkki: "Directional Audio Coding in Spatial Sound Reproduction and Stereo Upmixing," AES 28th International Conference, Pitea, Sweden, 2006.

[16] F. Zotter and H. Pomberger: "Warping the Recording Angle in Ambisonics," ICSA 2011, Detmold, Germany, 2011.

[17] V. Pulkki: "Localization of Amplitude-Panned Virtual Sources II: Two- and Three-Dimensional Panning," J. Audio Eng. Soc., Vol. 49, No. 9, 2001.